Astronomy & Astrophysics manuscript no. main
April 3, 2024

COSMOGLOBE DR2. II. Bayesian global modelling of zodiacal light with a first application to COBE-DIRBE

M. San et al.

Institute of Theoretical Astrophysics, University of Oslo, Blindern, Oslo, Norway

April 3, 2024

ABSTRACT

We present the first Bayesian framework for global modeling of zodiacal light in the time domain and its application to the Diffuse Infrared Background Experiment (DIRBE) time-ordered data. These data are first reanalyzed globally along with data from Planck HFI, COBE-FIRAS, GAIA, and WISE within the COSMOGLOBE framework, using the Kelsall et al. 1998 (K98) zodiacal light model to reproduce the zodiacal light subtractions from the official DIRBE analysis. We then re-estimate the exact zodiacal light parameters fit in the DIRBE analysis and show that we achieve better-determined zero-levels and lower zodiacal light residuals through our global Bayesian analysis. Finally, by generalizing the K98 model and incorporating various features from the Rowan-Robinson and May 2013 (RRM) model, we demonstrate that one can significantly improve current state-of-the-art zodiacal light models with existing archival data. A big step towards building better zodiacal light models and opening the infrared spectrum up for cosmological analysis will be to integrate the AKARI and IRAS time-ordered data into this framework.

Key words. Zodiacal dust, Interplanetary medium, Cosmology: cosmic background radiation

Contents

1 Introduction 1

2 Zodiacal light modelling in Commander 2
2.1 Parameterization the interplanetary dust distribution . . . 2
2.2 Reference models . . . 2
2.2.1 DIRBE/Kelsall (K98) . . . 2
2.2.2 Rowan-Robinson and May (RRM) . . . 2
2.3 Radiative and scattering properties . . . 2
2.4 Line-of-sight integrals . . . 2
2.5 Geocentric stationary zodiacal light . . . 3

3 Bayesian zodiacal light parameter estimation 3
3.1 Data selection and masks . . . 3
3.2 Time-ordered sampling vs week maps . . . 3
3.3 Zodiacal light parameter atlas . . . 3
3.4 Gibbs sampling of zodiacal light parameters . . . 3

4 Improved zodiacal light models 3
4.1 Re-estimated DIRBE/K98 model . . . 3
4.2 Exploring alternative zodiacal light models . . . 3
4.2.1 Freeing up frozen K98 parameters . . . 3
4.2.2 Inclusion of more asteroidal dust bands . 3
4.2.3 The Rowan-Robinson and May parametrization . . . 3
4.2.4 Survey of zodiacal light parameter variations . . . 3

5 Conclusions 3

1. Introduction

Zodiacal light (ZL, sometimes zodiacal emission or interplanetary dust emission) is the primary source of diffuse radiation observed in the infrared sky between 1-100 μm (Leinert, Ch. et al. (1998) and references therein). The light comes from scattering and re-emission of sunlight from interplanetary dust (IPD) grains. ZL is usually the most difficult source of foreground contamination to remove in studies of the Extragalactic Background Light (EBL) due to its seasonal nature. As such, a big part of the infrared sky has been inaccessible to cosmological analysis, due to difficulties with ZL modeling. Improving our models of the interplanetary medium is on of the most crucial steps for large scale detections of the EBL.

Existing ZL model typically consists of a three-dimensional model for the IPD distribution in the Solar system, along with a description of the ZL brightness through the radiative and scattering properties of the IPD. The ZL observed by an instrument is then computed by evaluating the brightness along each observed line-of-sight. The state-of-the-art ZL model is the field of cosmology is the Kelsall et al. 1998(Kelsall et al. 1998) (K98), which was built by the DIRBE team for the purpose of removing ZL from their data in the late 1900s. Since then, our understanding of the infrared sky has improved drastically with experiments such as Planck HFI, Gaia, and WISE, giving us access to far superior sky models. These new models, along with computational advances in Bayesian cosmological analysis (BeyondPlanck Collaboration et al. 2023; Galloway et al. 2023; Watts et al. 2023), complimentary data in the infrared, and more compute power allows us to extract much more information about the true nature of the interplanetary medium from the DIRBE data then what was possible for the DIRBE team at the time.

In this paper we present the ZL modelling efforts in the COSMOGLOBE DR2 release. In Sect. 2, we give a brief overview of the ZL model and its implementation in Commander. In Sect. 3

we discuss sampling of ZL models and present new novel techniques. In Sect. 4 we present the new state-of-the-art ZL model obtained, which is a re-stimation of the the parameters in the K98 model with some additional modification, along with preliminary results from more comprehensive modifications to the ZL models achieved by generalizing the K98 model and incorporating various features from the Rowan-Robinson and May 2013 (RRM) model. Finally, we discuss the implications of these results and the future of ZL modeling in the COSMOGLOBE framework, with suggestions for better ZL modelling and which data sets to include in future studies.

2. Zodiacal light modelling in Commander

2.1. Parameterization the interplanetary dust distribution

The IPD distribution in the Zodiacal cloud is both smooth and stable. However, fine structures are produced within the smooth cloud from asteroidal collisions, cometary trails, and gravitational resonance in the orbit of the planets. The number density $n(x, y, z)$ of the total IPD at some heliocentric ecliptic position (x, y, x) can therefore be described as the sum of several spatially distinct IPD distributions. Each distinct distribution is called a zodiacal component, denoted by c. These components do not necessarily share a plane of symmetry with the smooth cloud. We therefore allow them to have an offset from the Sun $(x_{0,c}, y_{0,c}, z_{0,c})$ such that the component-centric coordinates become

$$\begin{aligned} x_c &= x - x_{0,c} \\ y_c &= y - y_{0,c} \\ z_c &= z - z_{0,c}. \end{aligned} \tag{1}$$

Similarly, the tilt and orientation of a zodiacal components symmetry plane can be described by its inclination i_c and ascending node Ω_c. In the these coordinates, the density of a zodiacal component is fully described by the radial distance from its origin r_c, and the height above the symmetry plane Z_c

$$r_c = \sqrt{x_c^2 + y_c^2 + z_c^2}, \tag{2}$$

$$Z_c = x_c \sin\Omega_c \sin i_c - y_c \cos\Omega_c \sin i_c + z_c \cos i_c. \tag{3}$$

2.2. Reference models

2.2.1. DIRBE/Kelsall (K98)

The K98 model consists of the following zodiacal components: 1) The diffuse cloud, representing the smooth component of the zodiacal cloud; 2) Three asteroidal dust bands; 3) The circumsolar ring, representing the dust trapped in the orbit of the Earth. In the region trailing the Earth, an enhancement is included in this ring known as the Earth-trailing feature. The parametrization of these components are listed below where n_{C}, n_{B_i}, n_{R} are the number densities of the diffuse cloud, asteroidal dust bands, and the circum-solar ring, respectively.

$$n_{\mathrm{C}}(x, y, z) = n_{0,\mathrm{C}} r_{\mathrm{C}}^{-\alpha} f(\zeta_{\mathrm{C}}), \tag{4}$$

$$n_{\mathrm{B}_i}(x, y, z) = \frac{3n_{0,\mathrm{B}_i}}{r_{\mathrm{B}_i}} \exp\left[-\left(\frac{\zeta_{\mathrm{B}_i}}{\delta_{\zeta_{\mathrm{B}_i}}}\right)^6\right]\left[1 + \left(\frac{\zeta_{\mathrm{B}_i}}{\delta_{\zeta_{\mathrm{B}_i}}}\right)^p v^{-1}\right] \tag{5}$$

$$\times\left\{1 - \exp\left[-\left(\frac{r_{\mathrm{B}_i}}{\delta_{r_{\mathrm{B}_i}}}\right)^{20}\right]\right\}, \tag{6}$$

$$n_{\mathrm{R}}(x, y, z, \theta) = n_{0,\mathrm{SR}} \exp\left[-\frac{(r_{\mathrm{R}} - r_{0,\mathrm{SR}})^2}{\sigma_{R,\mathrm{SR}}^2} - \frac{|Z_{\mathrm{R}}|}{\sigma_{Z,\mathrm{SR}}}\right], \tag{7}$$

$$+ n_{0,\mathrm{TF}} \exp\left[-\frac{(r_{\mathrm{R}} - r_{0,\mathrm{TF}})^2}{\sigma_{R,\mathrm{TF}}^2} - \frac{|Z_{\mathrm{F}}|}{\sigma_{Z,\mathrm{TF}}} - \frac{(\theta - \theta_{0,\mathrm{TF}})^2}{\sigma_{\theta,\mathrm{TF}}^2}\right]. \tag{8}$$

2.2.2. Rowan-Robinson and May (RRM)

The Rowan-Robinson model(Rowan-Robinson & May 2013) is a recent more physically motivated IPD model. It features the a fan component which represents the diffuse IPD distribution up until the orbit of mars, and then a cometary component which represents the diffuse IPD distribution beyond the orbit of Mars and until the asteroid belt. The model has asteroidal bands similar to K98, but in the RRM model they come in two categories: One pair of broad bands, and two narrow bands. The RRM model also includes a contribution from uniformly distributed interstellar dust. Rather than using Z_c, the height above the symmetry plane, the RRM parametrization uses $\beta_c = \arcsin|Z_c/r_c|$. The parametrization of the RRM model is as follows

$$n_{\mathrm{F}}(x, y, z) = n_{0,\mathrm{F}} r_{\mathrm{F}}^{-\gamma} f(\beta_0), \tag{9}$$

where

$$f(\beta_0) = \exp\left[-P|\sin\beta_0|\right]. \tag{10}$$

2.3. Radiative and scattering properties

The IPD grains are assumed to emit thermal emission on the form of a blackbody modified by an emissivity factor $E_{c,\lambda}$

$$I_{c,\lambda}^{\mathrm{Thermal}} = E_{c,\lambda} B_\lambda(T). \tag{11}$$

where $B_\lambda(T)$ is the Planck function. The temperature T of the IPD is assumed to fall off with radial distance from the Sun r on the form

$$T(r) = T_0 R^{-\delta}, \tag{12}$$

where δ is the power law index which is 0.5 for theoretical gray dust.

At wavelengths where $\lambda \sim$ the grain size, the sunlight will be scattered instead of absorbed by the IPD. The scattered

The scattered light is described by the solar flux $F_\lambda^\odot$, the phase function $\Phi_\lambda(\Theta)$ representing the probability of a photon being scattered at an angle Θ, and the reflectivity or albedo $A_{c,\lambda}$ of the dust grains

$$I_{c,\lambda}^{\mathrm{Scattering}} = A_{c,\lambda} F_\lambda^\odot(R) \Phi_\lambda(\Theta). \tag{13}$$

We refer to San et al. (2022) for a more details. The total intensity from the zodiacal light is then the sum of the scattered and thermal emission

$$I_{c,\lambda}^{\mathrm{Total}} = I_{c,\lambda}^{\mathrm{Scattering}} + I_{c,\lambda}^{\mathrm{Thermal}} \tag{14}$$

$$= A_{c,\lambda} F_\lambda^\odot(R) \Phi_\lambda(\Theta) + (1 - A_{c,\lambda}) E_{c,\lambda} B_\lambda(T(R)). \tag{15}$$

2.4. Line-of-sight integrals

When evaluating the zodiacal emission at a time t we integrating along a line-of-sight ds from the observer towards the observed pixel p

$$I_{p,t} = \sum_c \int n_c \left[A_{c,\lambda} F_\lambda^\odot \Phi_\lambda + (1 - A_{c,\lambda}) E_{c,\lambda} B_\lambda\right] \mathrm{ds}, \tag{16}$$

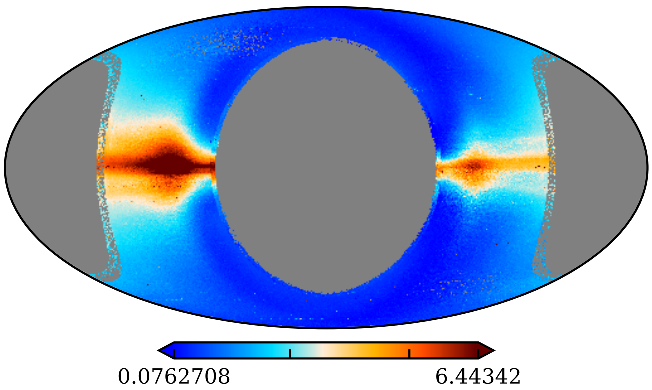

Fig. 1. Geocentric map $M_\nu^{\oplus}$ of the full survey, where we have subtracted away the sky model in addition to the diffuse cloud and the asteroidal dust bands. What we are left with is the stationary emission from the circumsolar ring and the Earth-trailing and possible other contamination from sidelobes.

2.5. Geocentric stationary zodiacal light

The circumsolar-ring and Earth-trailing feature are by definition distributed with respect to the Earth. In an Earth-centric, or geocentric, reference frame, the signal from such components will be stationary on the sky, if these are infact perfectly following the Earth around in the orbit. We can therefore make a geocentric map of the full survey, where we have subtracted away the sky model in addition to the diffuse cloud and the asteroidal dust bands. What we are left with is the static zodiacal emission coming from the circumsolar ring and the Earth-trailing feature and other potential earth centric interplanetary dust. This map can then be used as a lookup map for the combined emission from the circumsolar ring and the Earth-trailing feature components. The projection of the signal from this map to the timestream at a DIRBE frequency ν, at a pixel p in galactic coordinates, and at at a time t is then a matter of a simple lookup

$$S_{\nu,t,p}^{\mathrm{Ring+Feature}} = M_{\nu,p'}^{\oplus}, \tag{17}$$

where $M_{\nu,p'}^{\oplus}$ is the geocentric lookup map and p' is the corresponding pixel index in the geocentric reference frame. An example of such a map is shown in figure 1.

3. Bayesian zodiacal light parameter estimation

3.1. Data selection and masks

3.2. Time-ordered sampling vs week maps

3.3. Zodiacal light parameter atlas

3.4. Gibbs sampling of zodiacal light parameters

4. Improved zodiacal light models

4.1. Re-estimated DIRBE/K98 model

4.2. Exploring alternative zodiacal light models

4.2.1. Freeing up frozen K98 parameters

4.2.2. Inclusion of more asteroidal dust bands

4.2.3. The Rowan-Robinson and May parametrization

4.2.4. Survey of zodiacal light parameter variations

5. Conclusions

Acknowledgements. The current work has received funding from the European Union's Horizon 2020 research and innovation programme under grant agreement numbers 819478 (ERC; CosmoGlobe) and 772253 (ERC; bits2cosmology). Some of the results in this paper have been derived using the HEALPix (Górski et al. 2005) package. We acknowledge the use of the Legacy Archive for Microwave Background Data Analysis (LAMBDA), part of the High Energy Astrophysics Science Archive Center (HEASARC). HEASARC/LAMBDA is a service of the Astrophysics Science Division at the NASA Goddard Space Flight Center.

References

BeyondPlanck Collaboration, Andersen, K. J., Aurlien, R., et al. 2023, A&A, 675, A1
Galloway, M., Andersen, K. J., Aurlien, R., et al. 2023, A&A, 675, A3
Górski, K. M., Hivon, E., Banday, A. J., et al. 2005, ApJ, 622, 759
Kelsall, T., Weiland, J. L., Franz, B. A., et al. 1998, ApJ, 508, 44
Leinert, Ch., Bowyer, S., Haikala, L. K., et al. 1998, Astron. Astrophys. Suppl. Ser., 127, 1
Rowan-Robinson, M. & May, B. 2013, MNRAS, 429, 2894
San, M., Herman, D., Erikstad, G. B., Galloway, M., & Watts, D. 2022, A&A, 666, A107
Watts, D. J., Basyrov, A., Eskilt, J. R., et al. 2023, A&A, 679, A143

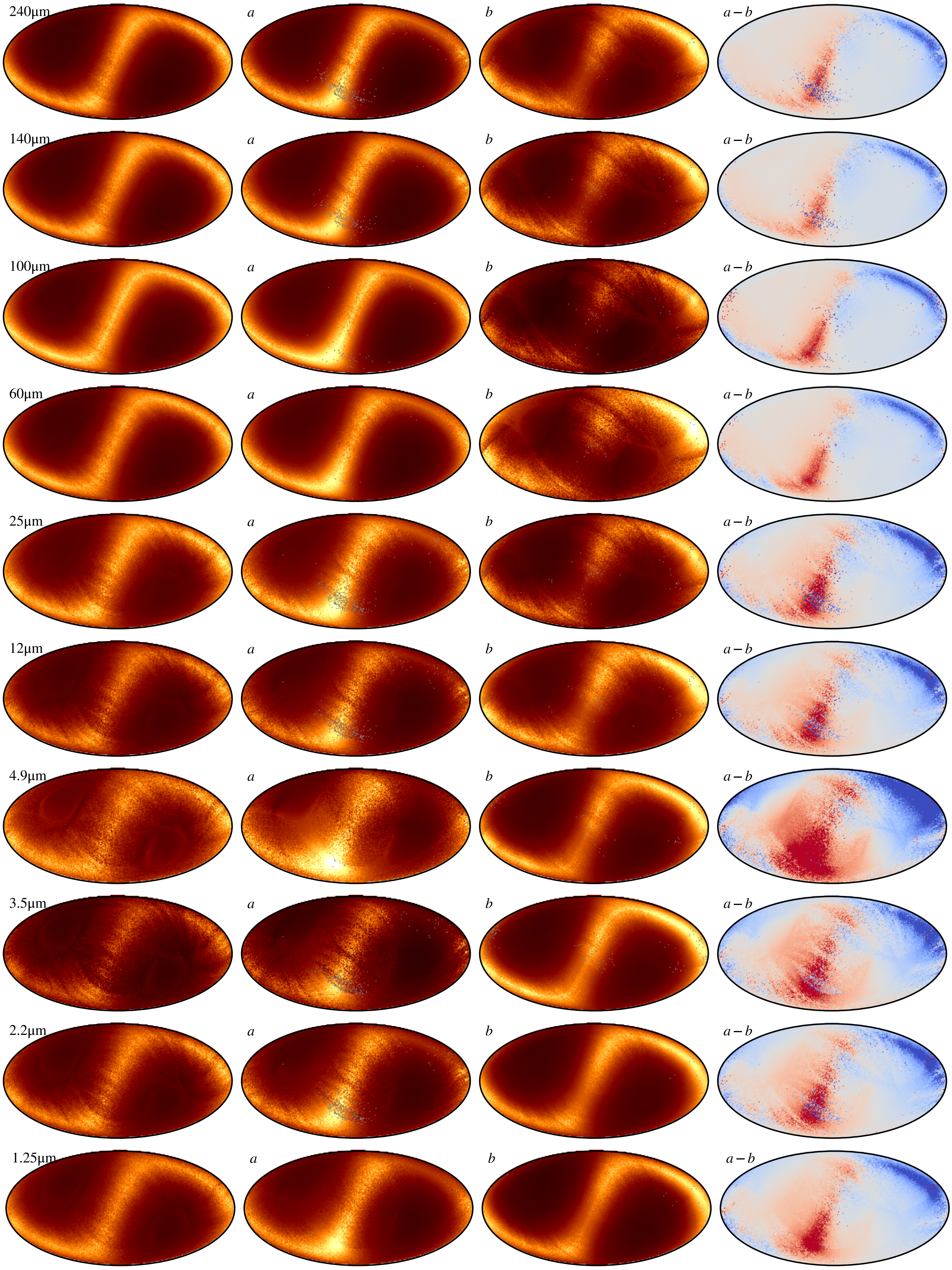

Fig. 2. Zodi frequency maps

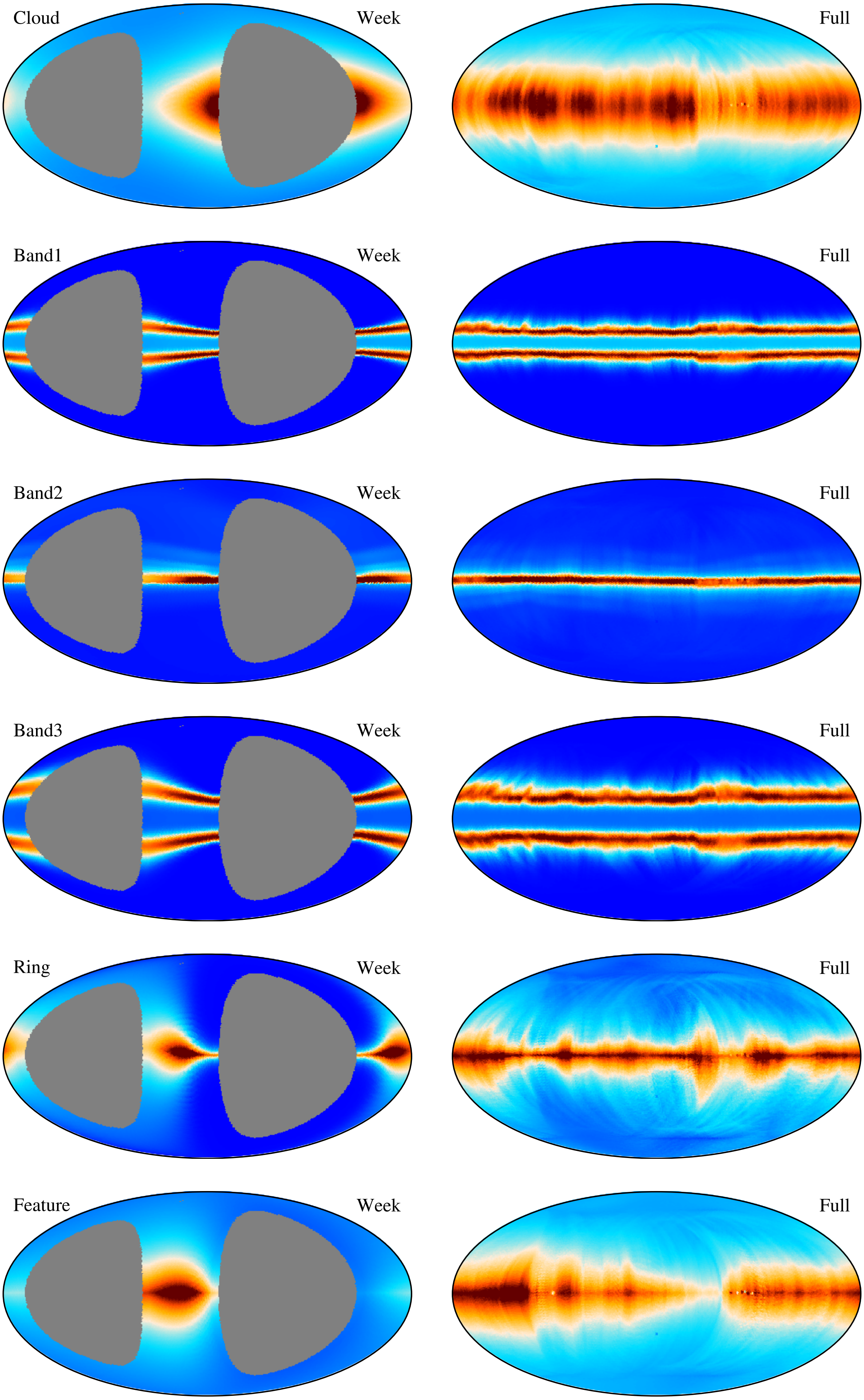

Fig. 3. week map of comps*

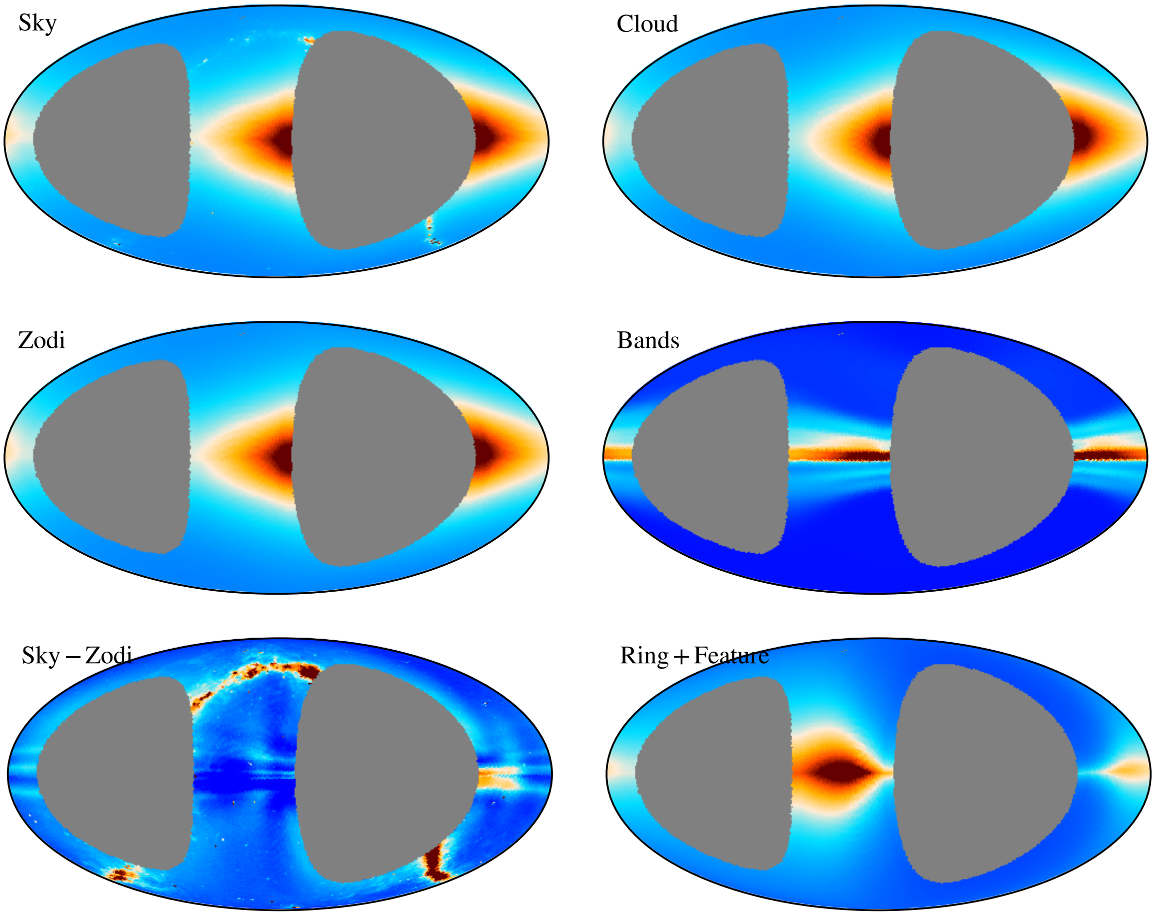

Fig. 4. week map of comps*